Proceedings of the 2005 IEEE
International Conference on Robotics and Automation
Barcelona, Spain, April 2005

On the Possibility of Excessive Internal Forces on Manipulated Objects in Robotic Contact Tasks

Yusuke MAEDA
Division of Systems Research, Faculty of Engineering,
Yokohama National University
79-5 Tokiwadai, Hodogaya-ku, Yokohama 240-8501, JAPAN
maeda@ynu.ac.jp

***Abstract*— In this paper, we study excessive internal forces applied to manipulated objects in robotic contact tasks. Such internal forces may cause serious damage to the objects and/or robots; thus, prior assessment of the possibility of excessive internal forces is very important.**

We propose a method to judge the possibility of excessive internal forces on manipulated objects. The judgment is based on rigid-body mechanics with Coulomb friction and given by solving a series of linear programming problems. We show some numerical examples of the judgment by our proposed method.

***Index Terms*— Internal Force, Robotic Contact Tasks, Linear Programming**

I. Introduction

In robotic contact tasks, excessive internal forces might be generated on objects in contact with the environment (Fig. 1). Especially when we use position-controlled robots, even minute positional errors of the robots may generate excessive internal forces on the objects, which leads to serious damage to the objects and/or the robots. Therefore, prior assessment of the possibility of excessive internal forces is highly important for planning and execution of robotic contact tasks. For example, in planning of graspless manipulation [1] (or nonprehensile manipulation [2]), appropriate assignment of position control and force control to robot fingers can be performed based on the assessment of the possibility of excessive internal forces [3].

Some related studies can be found in the field of assembly, fixturing, and robotic manipulation. Asada and By formulated the notion of "bilateral constraints" in the analysis of fixturing [4]. Bilateral constraints correspond to the possibility of excessive internal forces in frictionless cases, because normal forces of arbitrary magnitude by the contacts that form a bilateral constraint can cancel each other and be increased unlimitedly. Trinkle defined a class of equilibrium as "strong force closure," where grasped objects can be subject to unbounded contact wrench [5]. Frictionless strong force closure can be tested by linear programming. Hirai and Asada presented an algorithm to judge the existence of bilateral constraints based on the theory of polyhedral convex cones [6]. Bicchi showed that "internal passive contact forces," which include excessive internal forces, exist in the intersection of the null space of grasp matrix and that of the transpose of hand Jacobian matrix [7].

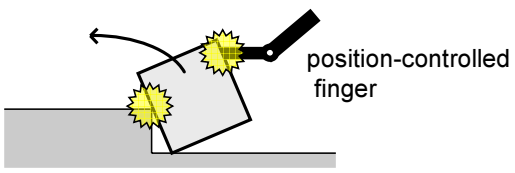

Fig. 1. Excessive Internal Force

The authors presented a method to judge the possibility of excessive internal forces on objects in robotic contact tasks with Coulomb friction [8]. The judgment is given by solving a linear programming problem based on rigid-body statics. However, the method tests only a weak necessary condition; it sometimes says that there is a danger of excessive internal forces even when they could not be generated (see examples in Section V). This is because the method does not consider some constraints on static frictional forces at the contacts.

In this paper, we present a method for more accurate judgment of the possibility of excessive internal forces than our previous one. The new method is based on the constraints on static frictional forces that were originally derived by Omata and Nagata [9] [10] for power grasps.

II. Problem Statement

A. Assumptions

Let us consider robotic contact tasks as shown in Fig. 2, where an object in contact with the environment is manipulated by robots.

We make the following assumptions to investigate excessive internal forces on the manipulated object:

1) The object, end-effectors of the robots, and the environment are rigid.
2) All the contacts can be approximated by finite point contacts.
3) Static Coulomb friction exists at the contact points.
4) Each of friction cones at the contacts can be approximated by a polyhedral convex cone [6].
5) The robots are position-controlled or force-controlled.
6) The magnitude of joint torque of the position-controlled robots has no limit.

We perform mechanical analysis based on rigid-body statics with Coulomb friction.

B. Definition of "Excessive Internal Force"

We should make it clear what is "excessive internal force" before proceeding to mechanical analysis. In this paper, as same as in [8], infinite internal (generalized) forces are referred to as "excessive internal forces"; that is, when infinite internal forces can be exerted on the object, we say that "there is a possibility of excessive internal forces." When contact forces can be increased unlimitedly without breaking the balance of the forces, the object cannot escape from infinite (=excessive) internal forces.

Thus, the problem should be tackled here is how to judge whether infinite internal forces are possible or not based on rigid-body statics.

III. Mechanical Model

A. Contact Forces

Let $\boldsymbol{p}_1, \ldots, \boldsymbol{p}_M \in \Re^3$ be the positions of the contact points. The friction cone at the i-th contact point is approximated by a polyhedral convex cone with unit edge vectors, $\boldsymbol{c}_{i1}, \ldots, \boldsymbol{c}_{is} \in \Re^3$. Contact force at the i-th contact point, $\boldsymbol{f}_i (\in \Re^3)$, can be expressed as:

$$\boldsymbol{f}_i = \boldsymbol{C}_i \boldsymbol{k}_i \ (\boldsymbol{k}_i \geq \boldsymbol{0}), \tag{1}$$

where $\boldsymbol{C}_i := [\boldsymbol{c}_{i1} \ \ldots \ \boldsymbol{c}_{is}] \in \Re^{3\times s}$ and $\boldsymbol{k}_i := [k_{i1}, \ldots, k_{is}]^T \in \Re^s$.

We can usually ignore contact forces applied by force-controlled robots because most of them cannot contribute to the realization of infinite internal forces. However, force-controlled robots with defective contacts [7] [11] should be taken into consideration for the judgment of the possibility of excessive internal forces. This is because defective contacts may be able to apply contact forces of arbitrary magnitude in specific directions. Thus, we should consider contact forces of force-controlled robots that satisfy the following constraint:

$$\boldsymbol{J}_i^T \boldsymbol{f}_i = \boldsymbol{0}, \tag{2}$$

where $\boldsymbol{J}_i \in \Re^{3\times L_i}$ is the Jacobian matrix between the position of the i-th contact point and joint angles of the corresponding robot; L_i is the number of joints of the robot ($L_i = 0$ for the contacts with the environment).

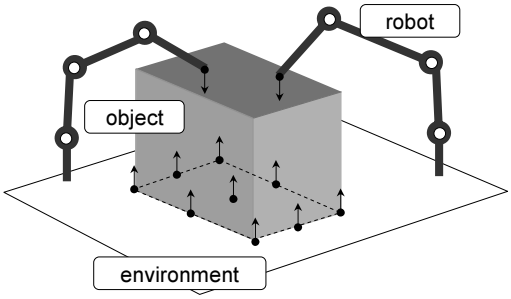

Fig. 2. Model of Robotic Contact Tasks

When the i-th contact is not defective (i.e., $\operatorname{rank} \boldsymbol{J}_i^T = 3$), $\dim \operatorname{Ker} \boldsymbol{J}_i^T = 0$ and therefore its contact force can be ignored for the judgment of the possibility of excessive internal forces.

Then we define the following matrices:

$$\boldsymbol{W} := \begin{bmatrix} \boldsymbol{I}_3 & \cdots & \boldsymbol{I}_3 \\ \boldsymbol{p}_1 \times \boldsymbol{I}_3 & \cdots & \boldsymbol{p}_M \times \boldsymbol{I}_3 \end{bmatrix} \in \Re^{6\times 3M}$$
$$\boldsymbol{C} := \operatorname{diag}(\boldsymbol{C}_1, \ldots, \boldsymbol{C}_M) \in \Re^{3M\times sM}$$
$$\boldsymbol{T} := \operatorname{diag}(\boldsymbol{T}_1, \ldots, \boldsymbol{T}_M) \in \Re^{3M\times 2M}$$
$$\boldsymbol{T}_i := [\boldsymbol{t}_{i1} \ \boldsymbol{t}_{i2}] \in \Re^{3\times 2}$$
$$\boldsymbol{J} := \operatorname{diag}(\boldsymbol{J}_1, \ldots, \boldsymbol{J}_M) \in \Re^{3M\times L},$$

where $\boldsymbol{I}_n$ is the $n \times n$ identity matrix; $\boldsymbol{p}_i \times \boldsymbol{I}_3 \in \Re^{3\times 3}$ is a skew-symmetric matrix defined such that $(\boldsymbol{p}_i \times \boldsymbol{I}_3)\boldsymbol{x} \equiv \boldsymbol{p}_i \times \boldsymbol{x}$; $\boldsymbol{t}_{i1}, \boldsymbol{t}_{i2} \in \Re^3$ are unit tangent vectors at the i-th contact defined such that $\boldsymbol{t}_{i1}^T \boldsymbol{t}_{i2} = 0$; $L := \sum_{i=1}^M L_i$.

Now all the contact forces can be represented as follows:

$$\boldsymbol{f} = \boldsymbol{C}\boldsymbol{k} \ (\boldsymbol{k} \geq \boldsymbol{0}), \tag{3}$$

where $\boldsymbol{f} := \left[\boldsymbol{f}_1^T, \ldots, \boldsymbol{f}_M^T\right]^T \in \Re^{3M}$ and $\boldsymbol{k} := \left[\boldsymbol{k}_1^T, \ldots, \boldsymbol{k}_M^T\right]^T \in \Re^{sM}$. All the tangential (=frictional) components of the contact forces are:

$$\boldsymbol{T}^T \boldsymbol{f} = \boldsymbol{T}^T \boldsymbol{C}\boldsymbol{k} \in \Re^{2M}. \tag{4}$$

The constraints for defective contacts of force-controlled robots (2) can be unified as follows:

$$\boldsymbol{J}^T \boldsymbol{A}\boldsymbol{f} = \boldsymbol{J}^T \boldsymbol{A}\boldsymbol{C}\boldsymbol{k} = \boldsymbol{0}, \tag{5}$$

where $\boldsymbol{A}$ is a selection matrix defined as:

$$\boldsymbol{A} := \operatorname{diag}(a_1 \boldsymbol{I}_3, \ldots, a_M \boldsymbol{I}_3) \in \Re^{3M\times 3M},$$
$$a_i := \begin{cases} 1 & \text{when the } i\text{-th contact corresponds to a force-controlled robot.} \\ 0 & \text{otherwise.} \end{cases}$$

When there are no force-controlled robots, $\boldsymbol{A} = \boldsymbol{O}$, and therefore the constraint (5) can be omitted.

The resultant force/moment applied to the object by all the contact forces that can contribute to the realization of infinite internal forces is given by:

$$\boldsymbol{W}\boldsymbol{f} = \boldsymbol{W}\boldsymbol{C}\boldsymbol{k} \in \Re^6. \tag{6}$$

B. Global Constraints on Possible Contact Forces

Static frictional forces on the contact points represented as (4) satisfy "local" constraints imposed by Coulomb's law. There exist, however, additional "global" constraints imposed by contact kinematics, which were derived by Omata and Nagata [9] [10] for power grasps. Here we show these additional constraints, which are slightly modified from the original formulation in [9] and [10] due to the application to robotic contact tasks instead of power grasps.

Let us consider a *virtual* infinitesimal motion of the object and the robots that causes sliding at some contact points. Note that this virtual motion is required only to derive the constraints on *static* frictional forces.

We define a selection matrix that selects contact points that will slide by the virtual motion as follows:

$$\boldsymbol{B} := \mathrm{diag}(b_1\boldsymbol{I}_3, \ldots, b_M\boldsymbol{I}_3) \in \Re^{3M\times 3M}, \tag{7}$$

where

$$b_i := \begin{cases} 1 & \text{when the } i\text{-th contact point will slide,} \\ 0 & \text{otherwise.} \end{cases}$$

From contact kinematics, the virtual motion corresponding to $\boldsymbol{B}$ must satisfy the following constraint [10]:

$$\boldsymbol{B}\begin{bmatrix}\boldsymbol{W}^T & \boldsymbol{J}\end{bmatrix}\begin{bmatrix}\boldsymbol{V} \\ -\dot{\boldsymbol{\theta}}\end{bmatrix} = \boldsymbol{T}\dot{\boldsymbol{Y}}, \tag{8}$$

where $\boldsymbol{V} = [\boldsymbol{v}^T \ \boldsymbol{\omega}^T]^T \in \Re^6$ is the (virtual) velocity/angular velocity of the object; $\dot{\boldsymbol{\theta}} = \left[\dot{\boldsymbol{\theta}}_1^T, \ldots, \dot{\boldsymbol{\theta}}_M^T\right]^T \in \Re^L$ and $\dot{\boldsymbol{\theta}}_i \in \Re^{L_i}$ is the (virtual) joint velocity vector of the robot corresponding to the i-th contact; $\dot{\boldsymbol{Y}} := \left[\dot{\boldsymbol{Y}}_1^T, \ldots, \dot{\boldsymbol{Y}}_M^T\right]^T \in \Re^{2M}$ and $\dot{\boldsymbol{Y}}_i \in \Re^2$ is the elements of the (virtual) sliding velocity vector at the i-th contact point (i.e., $\boldsymbol{T}_i\dot{\boldsymbol{Y}}_i$ is the sliding velocity vector). For convenience, let $\dot{\boldsymbol{Y}}_i = [0, 0]^T$ for contact points that are not selected by $\boldsymbol{B}$.

Equation (8) constrains the possible $\dot{\boldsymbol{Y}}$; thus, the possible signs of the elements of $\dot{\boldsymbol{Y}}$ are restricted. The possible signs of the elements of frictional forces, $\boldsymbol{T}^T\boldsymbol{C}\boldsymbol{k}$, are also restricted, because static frictional forces can apply only in the directions that prevent sliding.

Concretely, a combination of the signs of the elements of $\boldsymbol{T}^T\boldsymbol{C}\boldsymbol{k}$ is impossible if there exists no $\boldsymbol{B}$ that satisfies (8) for $\dot{\boldsymbol{Y}}$ whose elements have the same combination of their signs as $\boldsymbol{T}^T\boldsymbol{C}\boldsymbol{k}$. In other words, only $\boldsymbol{T}^T\boldsymbol{C}\boldsymbol{k}$ whose elements have the same combination of their signs as $\dot{\boldsymbol{Y}}$ that satisfies (8) is compatible with rigid-body motion.

Let us denote the set of frictional forces that satisfy the above constraint on the signs of the elements by $\boldsymbol{\mathcal{F}}$ and we have

$$\boldsymbol{T}^T\boldsymbol{C}\boldsymbol{k} \in \boldsymbol{\mathcal{F}}. \tag{9}$$

Note again that we consider not actual sliding but only virtual sliding in this paper, as well as [9] and [10]. Thus, the above constraint (9) is that on static frictional forces *before* sliding; it is different from constraints on kinetic frictional forces *in* sliding, which are dealt with in many papers such as [12].

IV. Judgment of the Possibility of Excessive Internal Forces

A. Formulation

In our previous method [8], the judgment of the possibility of excessive internal forces is given by the following linear programming problem:

$$\text{maximize } \mathbf{1}^T\boldsymbol{k} \quad \text{subject to} \begin{cases} \boldsymbol{W}\boldsymbol{C}\boldsymbol{k} = \boldsymbol{0} \\ \boldsymbol{J}^T\boldsymbol{A}\boldsymbol{C}\boldsymbol{k} = \boldsymbol{0} \\ \boldsymbol{k} \geq \boldsymbol{0}, \end{cases} \tag{10}$$

where $\mathbf{1} = [1, \ldots, 1]^T \in \Re^{sM}$. When $\boldsymbol{W}\boldsymbol{C}\boldsymbol{k} = \boldsymbol{0}$, contact forces can balance one another. If $\mathbf{1}^T\boldsymbol{k} \to \infty$, the contact forces can be infinite without breaking the force balance; consequently, there is a possibility of excessive internal forces. Otherwise, $\mathbf{1}^T\boldsymbol{k} = 0$ and there is no possibility of excessive internal forces.

However, the above judgment does not consider the constraint on static frictional forces described in Section III-B. When we take the constraint (9) into account, we should solve the following mathematical programming problem instead of (10):

$$\text{maximize } \mathbf{1}^T\boldsymbol{k} \quad \text{subject to} \begin{cases} \boldsymbol{W}\boldsymbol{C}\boldsymbol{k} = \boldsymbol{0} \\ \boldsymbol{J}^T\boldsymbol{A}\boldsymbol{C}\boldsymbol{k} = \boldsymbol{0} \\ \boldsymbol{T}^T\boldsymbol{C}\boldsymbol{k} \in \boldsymbol{\mathcal{F}} \\ \boldsymbol{k} \geq \boldsymbol{0}. \end{cases} \tag{11}$$

B. Algorithm for Judgment

It is not straightforward to solve (11) directly because $\boldsymbol{\mathcal{F}}$ in the constraints makes the problem nonlinear. Thus, we divide (11) into subproblems that have linear constraints so that we can judge the possibility of excessive internal forces by solving a series of linear programming problems.

To define the subproblems based on the signs of the elements of virtual sliding, we introduce the following matrix:

$$\boldsymbol{S} := \mathrm{diag}(s_{11},\ s_{12},\ s_{21},\ s_{22}, \ldots, s_{M1},\ s_{M2}) \in \Re^{2M\times 2M},$$

where

$$s_{ij} := \begin{cases} +1 & \text{when } b_i = 1 \text{ and the sign of the } j\text{-th element of } \dot{\boldsymbol{Y}}_i \text{ is positive,} \\ -1 & \text{when } b_i = 1 \text{ and the sign of the } j\text{-th element of } \dot{\boldsymbol{Y}}_i \text{ is negative,} \\ 0 & \text{when } b_i = 0. \end{cases}$$

Then we have:

$$\dot{\boldsymbol{Y}} = \boldsymbol{S}\boldsymbol{q}, \tag{12}$$

where $\boldsymbol{q}(\in \Re^{2M}) > \boldsymbol{0}$.

For a subcase specified by $\boldsymbol{S}$, we can judge the possibility of excessive internal forces by solving the following linear programming problem:

$$\text{maximize } \mathbf{1}^T\boldsymbol{k} \quad \text{subject to} \begin{cases} \boldsymbol{W}\boldsymbol{C}\boldsymbol{k} = \boldsymbol{0} \\ \boldsymbol{J}^T\boldsymbol{A}\boldsymbol{C}\boldsymbol{k} = \boldsymbol{0} \\ \boldsymbol{S}\boldsymbol{T}^T\boldsymbol{C}\boldsymbol{k} \leq \boldsymbol{0} \\ \boldsymbol{T}^T(\boldsymbol{I}_{3M} - \boldsymbol{B})\boldsymbol{C}\boldsymbol{k} = \boldsymbol{0} \\ \boldsymbol{k} \geq \boldsymbol{0}. \end{cases} \tag{13}$$

The constraint $\boldsymbol{S}\boldsymbol{T}^T\boldsymbol{C}\boldsymbol{k} \leq \boldsymbol{0}$ is added to represent (9). $\boldsymbol{T}^T(\boldsymbol{I}_{3M} - \boldsymbol{B})\boldsymbol{C}\boldsymbol{k} = \boldsymbol{0}$ means that the contact points that are not chosen by $\boldsymbol{B}$ cannot apply frictional forces. As same as the problem (10), there is a possibility of excessive internal forces when $\mathbf{1}^T\boldsymbol{k} \to \infty$.

Now we can present a naive algorithm for the judgment of the possibility of excessive internal forces as follows:

Step 1. Assume a combination of sliding/non-sliding contact points (namely, determine a selection matrix $\boldsymbol{B}$).

Step 2. Enumerate all the possible $\boldsymbol{S}$ for the specified $\boldsymbol{B}$ from the constraint (8). There are 2^{2n} patterns for $\boldsymbol{S}$ at most when $\boldsymbol{B}$ selects n sliding points.

Step 3. Judge the possibility of excessive internal forces for all the possible $\boldsymbol{S}$ by solving the problem (13). If there is a possibility of excessive internal forces for a possible $\boldsymbol{S}$, stop. Otherwise, go back to Step 1.

Step 4. If all the possible $\boldsymbol{B}$ have been checked, stop. In this case, there is no possibility of excessive internal forces.

Considering the constraints on frictional forces (9), the above procedure enables us to judge the possibility of excessive internal forces more accurately than our previous method [8].

If we implement the above procedure straightforwardly, we have to solve $5^M (= \sum_{n=0}^{M} {}_M C_n 2^{2n})$ linear programming problems at most. However, we can accelerate the judging procedure by using relaxation problems.

For example, when the result of the problem (10) indicates that there is no possibility of excessive internal forces, we have to solve none of the problems (13). This is because the problem (10) is a relaxation problem of (11). Similarly, we can also use the following relaxation problem of (13)

$$\text{maximize } \mathbf{1}^T \boldsymbol{k}$$
$$\text{subject to } \begin{cases} \boldsymbol{W}\boldsymbol{C}\boldsymbol{k} = \boldsymbol{0} \\ \boldsymbol{J}^T \boldsymbol{A}\boldsymbol{C}\boldsymbol{k} = \boldsymbol{0} \\ \boldsymbol{T}^T (\boldsymbol{I}_{3M} - \boldsymbol{B})\boldsymbol{C}\boldsymbol{k} = \boldsymbol{0} \\ \boldsymbol{k} \geq \boldsymbol{0}. \end{cases} \tag{14}$$

If $\mathbf{1}^T \boldsymbol{k} = 0$ in (14), we can skip Step 2 and 3 for the specified $\boldsymbol{B}$.

V. Numerical Examples

Let us present some numerical examples to explain how our method works. We implemented the judgment algorithm described in Section IV-B on Scilab. The computation times for the examples below are measured on a Linux PC with Celeron at 2.4 GHz.

For simplicity, we describe planar cases in detail, while very brief results are shown for spatial cases. For planar cases, we can use almost the same formulation as that in Section III and IV as follows:

$$\boldsymbol{p}_1, \ldots, \boldsymbol{p}_M \in \Re^2$$
$$\boldsymbol{f}_i = \boldsymbol{C}_i \boldsymbol{k}_i \in \Re^2 \ (\boldsymbol{k}_i \geq \boldsymbol{0})$$
$$\boldsymbol{C}_i := [\boldsymbol{c}_{i1} \ \boldsymbol{c}_{i2}] \in \Re^{2\times 2}; \ \boldsymbol{c}_{i1}, \boldsymbol{c}_{i2} \in \Re^2$$
$$\boldsymbol{k}_i := [k_{i1}, k_{i2}]^T \in \Re^2$$
$$\boldsymbol{f} := \left[\boldsymbol{f}_1^T, \ldots, \boldsymbol{f}_M^T\right]^T \in \Re^{2M}$$
$$\boldsymbol{k} := \left[\boldsymbol{k}_1^T, \ldots, \boldsymbol{k}_M^T\right]^T \in \Re^{2M}$$
$$\boldsymbol{W} := \begin{bmatrix} \boldsymbol{I}_2 & \cdots & \boldsymbol{I}_2 \\ \boldsymbol{p}_1 \times \boldsymbol{I}_2 & \cdots & \boldsymbol{p}_M \times \boldsymbol{I}_2 \end{bmatrix} \in \Re^{3\times 2M}$$

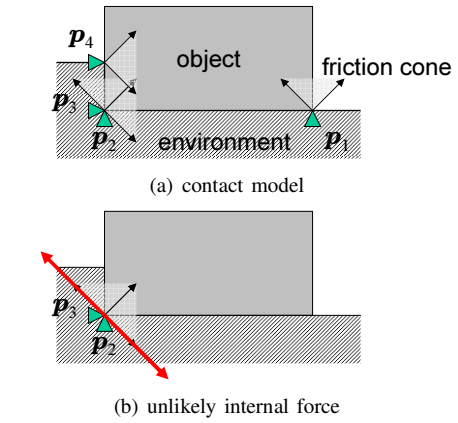

(a) contact model

(b) unlikely internal force

Fig. 3. Example: Object in Contact with a Corner (Planar Case)

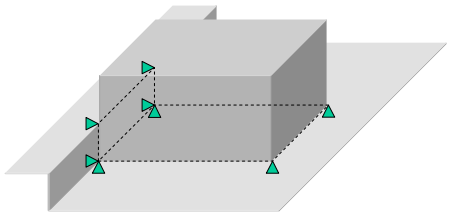

Fig. 4. Object in Contact with a Corner (Spatial Case)

$$\boldsymbol{C} := \mathrm{diag}(\boldsymbol{C}_1, \ldots, \boldsymbol{C}_M) \in \Re^{2M\times 2M}$$
$$\boldsymbol{T} := \mathrm{diag}(\boldsymbol{t}_1, \ldots, \boldsymbol{t}_M) \in \Re^{2M\times M}$$
$$\boldsymbol{J} := \mathrm{diag}(\boldsymbol{J}_1, \ldots, \boldsymbol{J}_M) \in \Re^{2M\times L}$$
$$\boldsymbol{A} := \mathrm{diag}(a_1 \boldsymbol{I}_2, \ldots, a_M \boldsymbol{I}_2) \in \Re^{2M\times 2M}$$
$$\boldsymbol{B} := \mathrm{diag}(b_1 \boldsymbol{I}_2, \ldots, b_M \boldsymbol{I}_2) \in \Re^{2M\times 2M}$$
$$\boldsymbol{S} := \mathrm{diag}(s_{11}, \ldots, s_{M1}) \in \Re^{M\times M},$$

where $\boldsymbol{p}_i \times \boldsymbol{I}_2 \in \Re^{1\times 2}$ is a matrix defined such that $(\boldsymbol{p}_i \times \boldsymbol{I}_2)\boldsymbol{x} \equiv \boldsymbol{p}_i \times \boldsymbol{x}$; $\boldsymbol{t}_i \in \Re^2$ is a unit tangent vector at the i-th contact.

A. An Object on a Corner

Consider a rectangular object on a right-angle corner as shown in Fig. 3. In this case, there are no robots and therefore we can ignore $\boldsymbol{J}$ and $\boldsymbol{\theta}$.

The static friction coefficient between the object and the environment (corner) is 1.0. We model the contact as four point contacts as depicted in Fig. 3(a). We set a reference frame whose origin coincides with the centroid of the object, then we have

$$\boldsymbol{p}_1 = \begin{bmatrix} 2 \\ -1 \end{bmatrix}, \ \boldsymbol{p}_2 = \boldsymbol{p}_3 = \begin{bmatrix} -2 \\ -1 \end{bmatrix}, \ \boldsymbol{p}_4 = \begin{bmatrix} -2 \\ 0 \end{bmatrix};$$
$$\boldsymbol{t}_1 = \boldsymbol{t}_2 = \begin{bmatrix} 1 \\ 0 \end{bmatrix}, \ \boldsymbol{t}_3 = \boldsymbol{t}_4 = \begin{bmatrix} 0 \\ -1 \end{bmatrix};$$
$$\boldsymbol{c}_{11} = \boldsymbol{c}_{21} = \frac{1}{\sqrt{2}} \begin{bmatrix} 1 \\ 1 \end{bmatrix}, \ \boldsymbol{c}_{12} = \boldsymbol{c}_{22} = \frac{1}{\sqrt{2}} \begin{bmatrix} -1 \\ 1 \end{bmatrix},$$
$$\boldsymbol{c}_{31} = \boldsymbol{c}_{41} = \frac{1}{\sqrt{2}} \begin{bmatrix} 1 \\ -1 \end{bmatrix}, \ \boldsymbol{c}_{32} = \boldsymbol{c}_{42} = \frac{1}{\sqrt{2}} \begin{bmatrix} 1 \\ 1 \end{bmatrix}.$$

Thus, we can calculate the following matrices:

$$\boldsymbol{W} = \begin{bmatrix} 1 & 0 & 1 & 0 & 1 & 0 & 1 & 0 \\ 0 & 1 & 0 & 1 & 0 & 1 & 0 & 1 \\ 1 & 2 & 1 & -2 & 1 & -2 & 0 & -2 \end{bmatrix}$$

$$\boldsymbol{C} = \frac{1}{\sqrt{2}} \begin{bmatrix} 1 & -1 & 0 & 0 & 0 & 0 & 0 & 0 \\ 1 & 1 & 0 & 0 & 0 & 0 & 0 & 0 \\ 0 & 0 & 1 & -1 & 0 & 0 & 0 & 0 \\ 0 & 0 & 1 & 1 & 0 & 0 & 0 & 0 \\ 0 & 0 & 0 & 0 & 1 & 1 & 0 & 0 \\ 0 & 0 & 0 & 0 & -1 & 1 & 0 & 0 \\ 0 & 0 & 0 & 0 & 0 & 0 & 1 & 1 \\ 0 & 0 & 0 & 0 & 0 & 0 & -1 & 1 \end{bmatrix}$$

$$\boldsymbol{T} = \begin{bmatrix} 1 & 0 & 0 & 0 \\ 0 & 0 & 0 & 0 \\ 0 & 1 & 0 & 0 \\ 0 & 0 & 0 & 0 \\ 0 & 0 & 0 & 0 \\ 0 & 0 & -1 & 0 \\ 0 & 0 & 0 & 0 \\ 0 & 0 & 0 & -1 \end{bmatrix}.$$

In this case, the result of the problem (10) is $\mathbf{1}^T \boldsymbol{k} \to \infty$ and therefore our previous method [8] says that there is a possibility of excessive internal forces. The excessive internal forces correspond to the contact forces within the friction cones at $\boldsymbol{p}_2$ and $\boldsymbol{p}_3$ (as illustrated in Fig. 3(b)). It is, however, unlikely that such internal forces will be generated.

On the other hand, in our new method, we enumerate the combinations of $\boldsymbol{B}$ and $\boldsymbol{S}$ that satisfy (8) and (12) as follows:

$$\begin{aligned}
&\boldsymbol{B} = \mathrm{diag}(1,1,1,1,0,0,0,0), \quad &&\boldsymbol{S} = \pm\,\mathrm{diag}(1,1,0,0);\\
&\boldsymbol{B} = \mathrm{diag}(1,1,0,0,0,0,1,1), \quad &&\boldsymbol{S} = \pm\,\mathrm{diag}(1,0,0,1);\\
&\boldsymbol{B} = \mathrm{diag}(0,0,0,0,1,1,1,1), \quad &&\boldsymbol{S} = \pm\,\mathrm{diag}(0,0,1,1);\\
&\boldsymbol{B} = \mathrm{diag}(1,1,0,0,0,0,0,0), \quad &&\boldsymbol{S} = \pm\,\mathrm{diag}(1,0,0,0);\\
&\boldsymbol{B} = \mathrm{diag}(0,0,1,1,0,0,0,0), \quad &&\boldsymbol{S} = \pm\,\mathrm{diag}(0,1,0,0);\\
&\boldsymbol{B} = \mathrm{diag}(0,0,0,0,1,1,0,0), \quad &&\boldsymbol{S} = \pm\,\mathrm{diag}(0,0,1,0);\\
&\boldsymbol{B} = \mathrm{diag}(0,0,0,0,0,0,1,1), \quad &&\boldsymbol{S} = \pm\,\mathrm{diag}(0,0,0,1);\\
&\boldsymbol{B} = \mathrm{diag}(0,0,0,0,0,0,0,0), \quad &&\boldsymbol{S} = \quad\mathrm{diag}(0,0,0,0).
\end{aligned}$$

For any of the above combinations, the result of problem (13) is $\mathbf{1}^T \boldsymbol{k} = 0$ and therefore there is no possibility of excessive internal forces. This shows that our new method can judge the possibility of excessive internal forces more accurately than our previous one.

We also tested a spatial case as shown in Fig. 4, which is almost equivalent to the planar case of Fig. 3(a). It takes 600 CPU seconds for our program to say that there is no possibility of excessive internal forces.

B. Pinched Objects

Consider pinched rectangular objects as shown in Fig. 5. In the case of Fig. 5(a), the object has two contacts with the environment; in the case of Fig. 5(b), the object has one contact with the environment and another contact with a robot. The robot is position-controlled and therefore $\boldsymbol{A} = \mathrm{diag}\{0,0,0,0\}$. The static friction coefficient at the contacts is 1.0 in both cases.

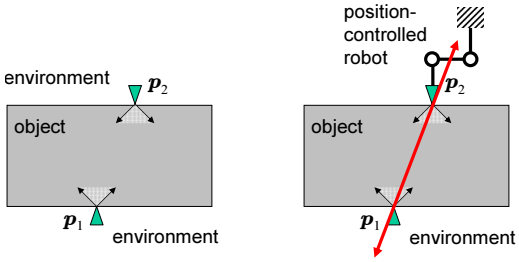

(a) pinched by environment (b) pinched by environment and robot

Fig. 5. Example: Pinched Objects (Planar Cases)

We set a reference frame whose origin coincides with the centroid of the object, then we have

$$\boldsymbol{p}_1 = \begin{bmatrix} -1 \\ -2 \end{bmatrix}, \ \boldsymbol{p}_2 = \begin{bmatrix} 1 \\ 2 \end{bmatrix};$$

$$\boldsymbol{t}_1 = \begin{bmatrix} 1 \\ 0 \end{bmatrix}, \ \boldsymbol{t}_2 = \begin{bmatrix} -1 \\ 0 \end{bmatrix};$$

$$\boldsymbol{c}_{11} = \frac{1}{\sqrt{2}} \begin{bmatrix} 1 \\ 1 \end{bmatrix}, \ \boldsymbol{c}_{12} = \frac{1}{\sqrt{2}} \begin{bmatrix} -1 \\ 1 \end{bmatrix},$$

$$\boldsymbol{c}_{21} = \frac{1}{\sqrt{2}} \begin{bmatrix} -1 \\ -1 \end{bmatrix}, \ \boldsymbol{c}_{22} = \frac{1}{\sqrt{2}} \begin{bmatrix} 1 \\ -1 \end{bmatrix}.$$

Thus, we can calculate the following matrices:

$$\boldsymbol{W} = \begin{bmatrix} 1 & 0 & 1 & 0 \\ 0 & 1 & 0 & 1 \\ 2 & -1 & -2 & 1 \end{bmatrix}$$

$$\boldsymbol{C} = \frac{1}{\sqrt{2}} \begin{bmatrix} 1 & -1 & 0 & 0 \\ 1 & 1 & 0 & 0 \\ 0 & 0 & -1 & 1 \\ 0 & 0 & -1 & -1 \end{bmatrix}$$

$$\boldsymbol{T} = \begin{bmatrix} 1 & 0 \\ 0 & 0 \\ 0 & -1 \\ 0 & 0 \end{bmatrix}.$$

We can ignore $\boldsymbol{J}$ and $\boldsymbol{\theta}$ in the case of Fig. 5(a). In the case of Fig. 5(b), let the position of the endpoint of the robot be

$$\begin{bmatrix} x \\ y \end{bmatrix} = \begin{bmatrix} \cos\theta_1 + \cos(\theta_1 + \theta_2) + 2 \\ \sin\theta_1 + \sin(\theta_1 + \theta_2) + 2 \end{bmatrix},$$

where θ_1 and θ_2 are the joint angles of the robot and $\theta_1 = \pi$, $\theta_2 = \pi/2$. Then we obtain

$$\begin{aligned}
\boldsymbol{J} &= \begin{bmatrix} 0 & 0 \\ 0 & 0 \\ -\sin(\theta_1) - \sin(\theta_1 + \theta_2) & -\sin(\theta_1 + \theta_2) \\ \cos(\theta_1) + \cos(\theta_1 + \theta_2) & \cos(\theta_1 + \theta_2) \end{bmatrix} \\
&= \begin{bmatrix} 0 & 0 \\ 0 & 0 \\ 1 & 1 \\ -1 & 0 \end{bmatrix}.
\end{aligned}$$

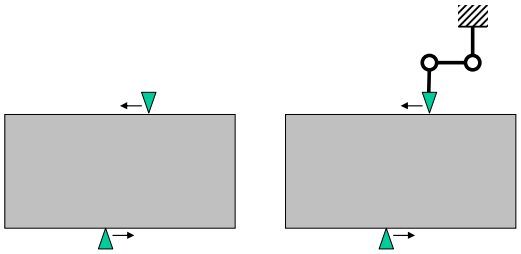

(a) incompatible virtual sliding (b) compatible virtual sliding

Fig. 6. Compatible/Incompatible Virtual Sliding

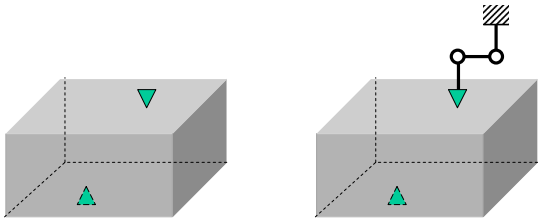

(a) pinched by environment (b) pinched by environment and robot

Fig. 7. Example: Pinched Objects (Spatial Cases)

Our previous method [8] cannot distinguish the cases of Fig. 5(a) and (b), and the result of the problem (10) is $\mathbf{1}^T \boldsymbol{k} \rightarrow \infty$. That is, the method says that there is a possibility of excessive internal forces for both cases.

On the other hand, in our new method, we enumerate the combinations of $\boldsymbol{B}$ and $\boldsymbol{S}$ that satisfy (8) and (12) for the case of Fig. 5(a) as follows:

$$\begin{aligned}
&\boldsymbol{B} = \mathrm{diag}(1,1,1,1), \quad &&\boldsymbol{S} = \pm\,\mathrm{diag}(1,-1);\\
&\boldsymbol{B} = \mathrm{diag}(1,1,0,0), \quad &&\boldsymbol{S} = \pm\,\mathrm{diag}(1,0);\\
&\boldsymbol{B} = \mathrm{diag}(0,0,1,1), \quad &&\boldsymbol{S} = \pm\,\mathrm{diag}(0,1);\\
&\boldsymbol{B} = \mathrm{diag}(0,0,0,0), \quad &&\boldsymbol{S} = \quad\ \mathrm{diag}(0,0).
\end{aligned}$$

For any of the above combinations, the result of the problem (13) is $\mathbf{1}^T \boldsymbol{k} = 0$ and therefore there is no possibility of excessive internal forces in the case of Fig. 5(a); recall that we deal with ideal rigid bodies and therefore no wedging forces occur in this case.

In the case of Fig. 5(b), the following combinations satisfy (8) and (12):

$$\begin{aligned}
&\boldsymbol{B} = \mathrm{diag}(1,1,1,1), \quad &&\boldsymbol{S} = \pm\,\mathrm{diag}(1,1);\\
&\boldsymbol{B} = \mathrm{diag}(1,1,1,1), \quad &&\boldsymbol{S} = \pm\,\mathrm{diag}(1,-1);\\
&\boldsymbol{B} = \mathrm{diag}(1,1,0,0), \quad &&\boldsymbol{S} = \pm\,\mathrm{diag}(1,0);\\
&\boldsymbol{B} = \mathrm{diag}(0,0,1,1), \quad &&\boldsymbol{S} = \pm\,\mathrm{diag}(0,1);\\
&\boldsymbol{B} = \mathrm{diag}(0,0,0,0), \quad &&\boldsymbol{S} = \quad\ \mathrm{diag}(0,0).
\end{aligned}$$

Because of the degrees of freedom of the robot, additional combinations, $\boldsymbol{B} = \mathrm{diag}(1,1,1,1)$ and $\boldsymbol{S} = \pm\,\mathrm{diag}(1,1)$, are allowed. That corresponds to the fact that a virtual sliding depicted in Fig. 6 is incompatible with rigid-body motion in the case of Fig. 5(a) while it is compatible in the case of Fig. 5(b). The result of the problem (13) in the case of Fig. 5(b) is $\mathbf{1}^T \boldsymbol{k} \rightarrow \infty$ when $\boldsymbol{B} = \mathrm{diag}(1,1,1,1)$ and $\boldsymbol{S} = -\,\mathrm{diag}(1,1)$, and therefore there is a possibility of excessive internal forces as illustrated in Fig. 5(b).

We also tested spatial cases as shown in Fig. 7, which are almost equivalent to the planar cases of Fig. 5. It takes 0.08 CPU seconds and 0.1 CPU seconds for Fig. 7(a) and Fig. 7(b), respectively, to judge the possibility of excessive internal forces.

VI. Conclusion

We presented a method to judge the possibility of excessive internal forces in robotic contact tasks by solving a series of linear programming problems. The method is an extended version of our previous one [8] and based on rigid-body statics. Numerical examples showed that the new method can judge the possibility of excessive internal forces more accurately than the old one. The improved accuracy results from the consideration of constraints on static frictional forces derived by Omata and Nagata [9] [10].

Developing more efficient judging procedure should be addressed in future work. This is very important for the application to manipulation planning [3] [13].

References

[1] Y. Aiyama, M. Inaba, and H. Inoue, "Pivoting: A new method of graspless manipulation of object by robot fingers," in *Proc. of IEEE/RSJ Int. Conf. on Intelligent Robots and Systems*, Yokohama, Japan, 1993, pp. 136–143.

[2] M. T. Mason, "Progress in nonprehensile manipulation," *Int. J. of Robotics Research*, vol. 18, no. 1, pp. 1129–1141, 1999.

[3] Y. Maeda and T. Arai, "Automatic determination of finger control modes for graspless manipulation," in *Proc. of IEEE/RSJ Int. Conf. on Intelligent Robots and Systems*, Las Vegas, NV, U.S.A., 2003, pp. 2660–2665.

[4] H. Asada and A. B. By, "Kinematic analysis of workpart fixturing for flexible assembly with automatically reconfigurable fixtures," *IEEE J. of Robotics and Automation*, vol. RA-1, no. 2, pp. 86–94, 1985.

[5] J. C. Trinkle, "On the stability and instantaneous velocity of grasped frictionless objects," *IEEE Trans. on Robotics and Automation*, vol. 8, no. 5, pp. 560–572, 1992.

[6] S. Hirai and H. Asada, "Kinematics and statics of manipulation using the theory of polyhedral convex cones," *Int. J. of Robotics Research*, vol. 12, no. 5, pp. 434–447, 1993.

[7] A. Bicchi, "On the problem of decomposing grasp and manipulation forces in multiple whole-limb manipulation," *Robotics and Autonomous Systems*, vol. 13, no. 2, pp. 127–147, 1994.

[8] Y. Maeda, Y. Aiyama, T. Arai, and T. Ozawa, "Analysis of object-stability and internal force in robotic contact tasks," in *Proc. of IEEE/RSJ Int. Conf. on Intelligent Robots and Systems*, Osaka, Japan, 1996, pp. 751–756.

[9] T. Omata and K. Nagata, "Rigid body analysis of the indeterminate grasp force in power grasps," *IEEE Trans. on Robotics and Automation*, vol. 16, no. 1, pp. 46–54, 2000.

[10] T. Omata, "Rigid body analysis of power grasps: Bounds of the indeterminate grasp force," in *Proc. of IEEE Int. Conf. on Robotics and Automation*, Seoul, Korea, 2001, pp. 2203–2209.

[11] X.-Y. Zhang, Y. Nakamura, and K. Yoshimoto, "Mechanical analysis of grasps with defective contacts using polyhedral convex set theory," *J. of Robotics Soc. of Japan*, vol. 14, no. 1, pp. 105–113, 1996, (in Japanese).

[12] J.-S. Pang and J. Trinkle, "Stability characterizations of rigid body contact problems with Coulomb friction," *Zeitschrift für Angewandte Mathematik und Mechanik*, vol. 80, no. 10, pp. 643–663, 2000.

[13] Y. Maeda, T. Nakamura, and T. Arai, "Motion planning of robot fingertips for graspless manipulation," in *Proc. of IEEE Int. Conf. on Robotics and Automation*, New Orleans, LA, U.S.A., 2004, pp. 2951–2956.